Pinning of charge and flux solitons in disordered Josephson junction arrays

Kirill G. Fedorov,[1,2,*] Mikhail V. Fistul,[3] and Alexey V. Ustinov[1,2]
[1]*Physikalisches Institut, Universität Karlsruhe, Karlsruhe, D-76131, Germany*
[2]*DFG-Center for Functional Nanostructures (CFN), D-76128 Karlsruhe, Germany*
[3]*Theoretische Physik III, Ruhr-Universität Bochum, D-44801 Bochum, Germany*
(Received 23 March 2011; published 28 July 2011)

We study the depinning of flux and charge solitons in discrete Josephson junction arrays with magnetic and charge inhomogeneities, respectively. The dependencies of soliton depinning force on the discreteness parameter a of the system and on the magnitude of disorder are calculated numerically and analytically. We obtain that for small values of discreteness ($a < 1$), magnetic (charge) inhomogeneities lead to a substantial increase of soliton depinning force with increasing the soliton size. In the opposite limit of $a \gtrsim 1$, the Peierls-Nabarro potential induced by discreteness of array, results in a strong decrease of the depinning force with the size of soliton. Thus, the dependence of pinning force on $1/a$ displays a pronounced minimum, and its position is determined by a strength of disorder. We find the optimal charge soliton size, which is favorable for overcoming pinning induced by disorder. In case of small but finite disorder, increase in the soliton size finally leads to a destruction of the soliton by strong spatial fluctuations.

DOI: 10.1103/PhysRevB.84.014526 PACS number(s): 74.50.+r, 85.25.−j

I. INTRODUCTION

Josephson coupled systems as parallel and series Josephson junction arrays meet with high interest due to their unique properties. One of these properties is the existence of topological flux solitons associated with vortices in long Josephson junctions and parallel Josephson arrays. Such a soliton (also called *fluxon*) carries a magnetic flux equal to the flux quantum $\Phi_0 = h/(2e) = 2.07 \cdot 10^{-15}$ Wb.[1,2] A single fluxon can travel along the junction with a maximum velocity about 30 times smaller than the speed of light in vacuum. Fluxons are used in many applications such as flux-flow oscillators,[3] frequency clocks[4] and qubit readout techniques.[5]

Due to the fundamental phase-charge duality in Josephson systems, analogous topological excitations dual to fluxons are assumed to exist in charge-governed series arrays of small Josephson junctions. These excitations are thought to be *charge solitons*, each of them carrying charge of a single Cooper pair.[6] Observation of such solitons might serve as another beautiful proof of the duality principle, and help to close the metrology triangle by implementing the charge-frequency standard.

Experimental efforts to search for charge solitons in arrays of Josephson junctions have not yet furnished direct evidence of their existence.[7–9] It is clear, that the interaction of a charge propagating through an array with static parasitic background charges is one of the major problems in such systems. This problem is common to all single electron devices, such as e.g. charge qubits and single electron transistors.[10–12] Background offset charges in the substrate induce randomly distributed electrical polarization in single-electron devices. Due to their extreme charge sensitivity spatial charge disorder results in a loss of functionality. It is extremely difficult to protect circuits against the influence of background charges in the substrate. However, there is hope to find regimes where the influence of parasitic disordered charges is negligible or, at least, minimal. Parasitic background charges in the substrate could result in strong pinning of charge solitons, which may effectively prevent their observation. In this paper, we will focus on the optimal range of parameters for making traveling charge solitons in discrete arrays of Josephson junctions insensitive to disorder. The main idea is that a Cooper pair charge soliton spread over many array's islands would not suffer from the locally trapped background charges as much as compact single-charge solitons do.

Flux solitons have less of a problem with pinning on random trapped fluxes due to the absence of spread magnetic monopoles. However, Abrikosov vortices, trapped in the superconducting electrodes of the junctions, can create exactly the same type of disorder for fluxons as background charges do for charge solitons. The depinning problem will be first discussed and solved for a well-known case of flux solitons and then mapped to the charge case. This approach is possible due to the duality principle between these two systems.

II. FLUX MODEL

One of the problems known to be associated with the practical use of fluxons in long junctions and parallel Josephson arrays (see Fig. 1(a)) is their pinning on random trapped magnetic fluxes. The random flux can be induced by e.g. by Abrikosov vortices randomly trapped in superconducting electrodes of the array (see Fig. 1(b)).[13–16] The pinned fluxon is in a metastable state until the bias current reaches a certain value at which the potential barrier vanishes and the fluxon escapes, switching a Josephson array from the superconducting to a finite voltage state. Thus, we are considering the depinning of a single fluxon in the presence of random fluxes spread along the array. This situation is different from the disorder models studied earlier, for instance,[17,18] dealing with the spread of local critical currents.

To describe the dynamics of magnetic flux in parallel Josephson junction arrays in the presence of *strong magnetic inhomogeneities*, the conventional perturbed sine-Gordon model is used, which take the presence of random trapped fluxes into account:

$$\frac{\partial^2\phi_i}{\partial t^2}+\alpha\frac{\partial\phi_i}{\partial t}-\frac{\phi_{i+1}-2\phi_i+\phi_{i-1}}{a^2}=\eta-\sin(\phi_i)+\theta_i-\theta_{i-1}, \tag{1}$$

here ϕ_i is the superconducting phase difference on the i-th junction, η is the bias current normalized to the critical current, α is the damping, $a = d/\lambda_J$ is the discreteness parameter, given by the distance between neighboring Josephson junctions d, normalized to the mean Josephson length λ_J, $\theta_i = I_i/I_c$ is the screening current created by the random flux Φ_i pinned in between the i-th and the $(i\text{-}1)$-th junction, normalized to the critical current I_c of the junction.

We take here an assumption that the maximum amplitude of possible random flux is equal to the half-flux quantum $\Phi_i = \Phi_0/2$. The reason for this constraint is that larger random fluxes would be accompanied by emerging fluxons propagating along the array.[19,20] These random fluxes Φ_i are homogeneously distributed in the range $-\Phi_A \leqslant \Phi_i \leqslant \Phi_A$ with the maximum possible disorder amplitude $\Phi_A = \Phi_0/2$. Let us now consider the case when both the amplitude of flux disorder Φ_A and critical current density per unit length j_c are independent of the discreteness parameter $a = d/\lambda_J$ of the array. This somewhat artificial condition allows to directly map the flux case to the charge system considered below.

A random current I_i is linked to a trapped flux Φ_i through $\Phi_i = LI_i$, where L is the inductance of a single array cell and the screening current I_i flows around it, as shown in Fig. 1. This can be rewritten as $\Phi_i = L\theta_i j_c d$. We notice that the inductance L is approximately proportional to the distance between junctions d. The deviation from this dependence is logarithmically small. Taking into account this functional dependence,

$$\frac{\Phi_i}{\Phi_0} = k \cdot \theta_i a^2, \tag{2}$$

results, where constant k is determined by the geometry of the array cells. Hence, keeping the flux disorder amplitude independent of the discreteness leads to the scaling of the respective screening currents θ_i inversely proportional to a^2. The same result is obtained in a more formal way when introducing a random flux in the perturbed sine-Gordon model by modifying the second order spatial finite difference as follows:

$$\frac{\phi_{i+1} - 2\phi_i + \phi_{i-1}}{a^2} \longrightarrow \frac{\phi_{i+1} - 2\phi_i + \phi_{i-1} + 2\pi(\Phi_i - \Phi_{i-1})/\Phi_0}{a^2}. \tag{3}$$

We choose the constant k in (2) to be $1/2\pi$. The chosen particular value of k does not restrict any dynamics, but just makes it easier to compare the flux and charge cases, as will be shown below. Thus, the normalized screening current θ_i inducing flux Φ_i is determined by the following expression:

$$\theta_i = \frac{2\pi\Phi_i}{a^2\Phi_0}. \tag{4}$$

In the absence of flux disorder, a fundamental pinning force of a soliton in a Josephson parallel array emerges from the so-called Peierls-Nabarro (PN) potential.[21] This potential is due to the restriction of arbitrary soliton translations along the array, i.e. shifts on a lattice spacing a and its integer multipliers are allowed only. The smallest energy barrier that soliton should overcome in order to start moving along the discrete array is the PN barrier, $E_{\mathrm{PN}} \approx A\exp(-B/a)$ (which is correct for $a < 1$), where A and B are constants and a is the discreteness parameter.[21] For the case of large discreteness the potential changes its form and in the limit of $a \gg 1$ becomes $E_{\mathrm{PN}} = 2 - \frac{\pi^2}{a^2}$.[21] Consequently, the energy barrier E_{PN} increases monotonically with a and becomes negligible in the limit of dense arrays, i.e. $a \ll 1$.

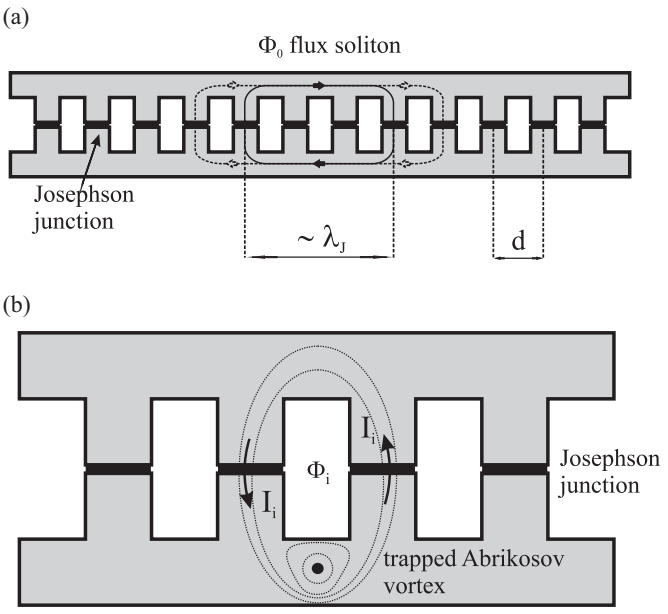

FIG. 1. (Color online) a) Schematic cross section of a discrete Josephson array with a fluxon inside. b) Schematic cross section of a discrete Josephson array with a trapped Abrikosov vortex creating a parasitic random current I_i.

III. CHARGE MODEL

In the dual case, we consider a series array of small Josephson junctions with randomly distributed trapped charges on the islands. The theoretical model of a charge-governed dynamics of this system has been developed in Refs. 6, 22, 23, 24, 25. In order to describe the dynamics of the Cooper-pair charge solitons in the array we employ the perturbed sine-Gordon equation with soliton mass determined by the Bloch-inductance L_B[24]:

$$L_B(q_i)\frac{\partial^2 q_i}{\partial t^2} + \frac{1}{2}\frac{\partial L_B(q_i)}{\partial q}\left(\frac{\partial q_i}{\partial t}\right)^2 + R\frac{\partial q_i}{\partial t} - \frac{q_{i+1} - 2q_i + q_{i-1}}{C_0} = V - \frac{2e}{C}\sin\left(\frac{\pi q_i}{e}\right), \tag{5}$$

where q_i is the charge variable (its physical meaning is the charge propagating through the i-th superconducting island[24]), V denotes the bias voltage, C is the capacitance of a single junction, C_0 is the capacitance of a superconducting grain to the ground (see Fig. 2), and R is the dissipative term responsible for the damping in charge arrays.

The static part of equations describing charge motion (5) in series arrays of superconducting grains can be mapped exactly to the static part of sine-Gordon equation (1), which describes the phase-governed junction array. The Josephson

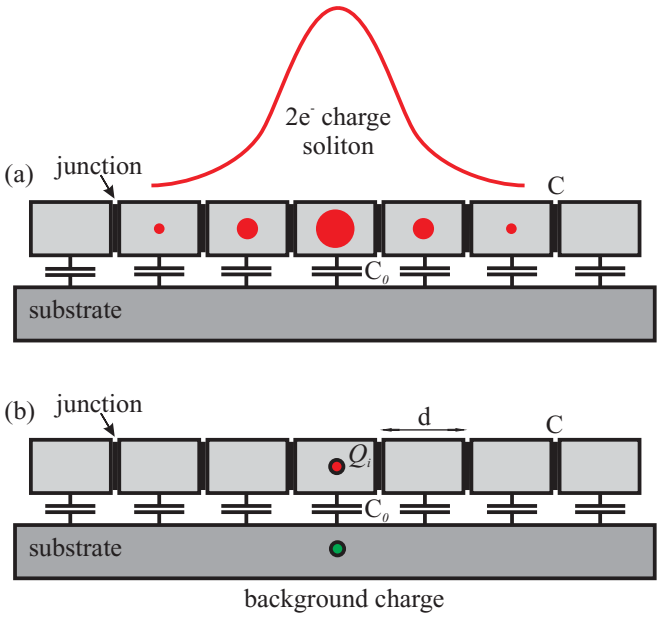

FIG. 2. (Color online) a) Schematic cross section of a series Josephson array with a presumable charge soliton inside. The soliton's charge distribution over several superconducting grains is colored red. b) Schematic cross section of the discrete junction array with a background charge inducing a parasitic charge on the superconducting island itself.

energy $E_J = \frac{I_c \Phi_0}{2\pi}$ here is considered to be equal to or larger than the charge energy $E_c = \frac{(2e)^2}{2C}$, i.e. $E_J \gtrsim E_C$. Under this condition, the Bloch inductance $L_B(q)$ is almost constant. Hence, mathematical descriptions for charge and flux sine-Gordon models fully coincide in this regime. This allows one to establish a direct mapping between the dynamics of Cooper-pair solitons in series arrays of superconducting grains and the dynamics of fluxons in parallel Josephson junction arrays.

In charge-governed series Josephson junction arrays, inhomogeneities are created by randomly trapped background charges in the substrate. These charges act through the capacitance of superconducting islands to the ground C_0 and induce parasitic polarization charges Q_i on the islands (see Fig. 2,b). These randomly distributed parasitic charges are obstacles for Cooper-pair tunneling. We take here an assumption that these charge offsets are randomly distributed in the range between $-Q_A$ and $+Q_A$, with the maximum possible amplitude equaling the single electron charge $Q_A = e$. The reason for this assumption is that charges higher than $|e|$ would be screened by single electrons tunneling across the junctions. In terms of Eq. (5), these polarization charges generate voltage drops $V_i = Q_i/C_0$ in the right part of the equation:

$$L_B(q_i)\frac{\partial^2 q_i}{\partial t^2} + \frac{1}{2}\frac{\partial L_B(q_i)}{\partial q}\left(\frac{\partial q_i}{\partial t}\right)^2 + R\frac{\partial q_i}{\partial t} - \frac{q_{i+1} - 2q_i + q_{i-1}}{C_0} = V - \frac{2e}{C}\sin\left(\frac{\pi q_i}{e}\right) + V_i - V_{i-1}, \quad (6)$$

In order to bring Eq. (6) to the same view as Eq. (1), the charge variable $q_i \to 2\pi q_i/(2e)$:

$$L_B^*(q_i)\frac{\partial^2 q_i}{\partial t^2} + \frac{1}{2}\frac{\partial L_B^*(q_i)}{\partial q}\left(\frac{\partial q_i}{\partial t}\right)^2 + R^*\frac{\partial q_i}{\partial t} - \frac{q_{i+1} - 2q_i + q_{i-1}}{a^2} = \nu - \sin(q_i) + \mu_i - \mu_{i-1}, \quad (7)$$

where

$$\mu_i = \frac{2\pi Q_i}{a^2 2e} \quad (8)$$

is the normalized random voltage on the i-th island and $\nu = VC/(2e)$. Usually, the voltage drop V (and, hence, ν) is strongly non-uniform along the system due to the screening of the external field applied at the array's boundaries. Nevertheless, ν is considered to be constant along the array to facilitate the mapping to Eq. (1). In an experiment such homogeneous voltage biasing can be achieved by a parallel chain of capacitors. Note, that the discreteness parameter a for charge junction arrays is given not just by the physical distance d (see Fig. 2) between the single junctions, but determined by the ratio of capacitances $a = \sqrt{C_0/C}$. The Peierls-Nabarro potential would occur in charge-governed arrays in same way it does in flux systems.

IV. NUMERICAL SIMULATIONS

We simulate the depinning of a single fluxon in a discrete Josephson array using Eq. (1) with the following constraints. The amplitude of random fluxes trapped between every pair of junctions is fixed. Fluxes are assumed to be uniformly distributed within the range $-\Phi_A \leqslant \Phi_i \leqslant \Phi_A$, where Φ_A is the maximum amplitude of a random flux. We define the disorder strength as $\gamma = 2\Phi_A/\Phi_0$. The corresponding constraint on random currents θ_i reads as $-\gamma\pi/a^2 < \theta_i < \gamma\pi/a^2$. Here, the case $\gamma = 1$ corresponds to the maximal random flux per cell equaling $\Phi_0/2$. The same condition applies to the charge case (8), with: $-\gamma\pi/a^2 < \mu_i < \gamma\pi/a^2$, where the case $\gamma = 1$ corresponds to the maximum possible induced charge equaling the single electron charge e.

In order not to confuse the reader by switching our presentation backwards and forwards between the two models, the setting will be explained below using the terms of the flux model, rather than the charge one. The results of the simulations, however, will be applicable to both the charge and the flux cases.

We calculate the depinning current using numerical simulations of the discrete sine-Gordon model (1) in the underdamped regime with $\alpha = 0.05$ and random currents induced by trapped fluxes. The numerical solution of Eq. (1) under the open boundary conditions is computed on the basis of the implicit finite-difference scheme. Typical values of the time discretization step are $\Delta t = 0.05 - 0.01$, the number of averaging over different random flux configurations is $N = 10^4$.

The simulations run as follows. First, the sine-Gordon equation is solved to yield a statically stable configuration with a single fluxon placed in the middle of Josephson junction array. Then, the bias current is increased step by step until the fluxon starts to move at a certain current $I_{\rm dep}$ and eventually reaches the boundary of system. At this moment, the fluxon is

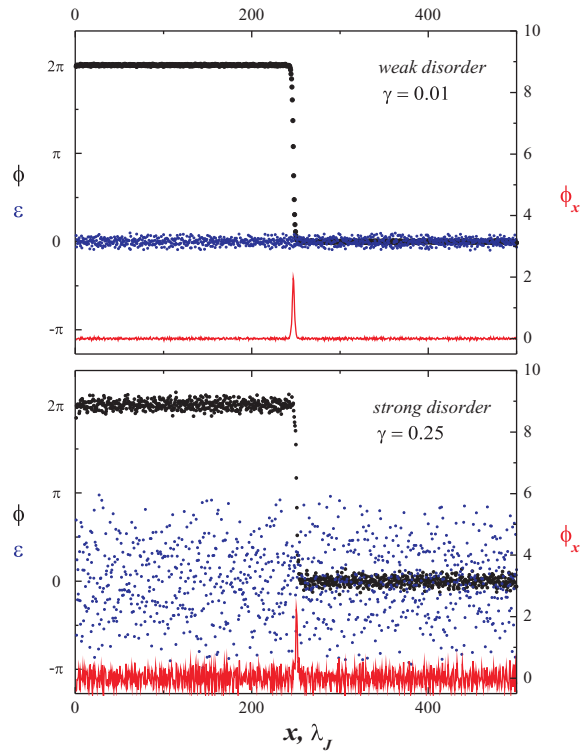

FIG. 3. (Color online) Fluxon (2π-kink) in the Josephson junction array with $a = 0.5$ at different disorder values γ. The same picture applies to 2e-solitons with the charge disorder. The black color here indicates the phase difference across the i-th junction ϕ_i, red - the spatial derivative over the phase difference, blue - the resulting random current $\varepsilon_i = \theta_i - \theta_{i-1}$.

completely depinned. To check the outcome, this simulation is repeated with a slower bias current ramping rate and for arrays of larger lengths. Once the depinning force obtained converges, we take the depinning bias value as the final result.

Fig. 3 shows the snapshots of the initial phase distribution with a soliton inside the array for weak and strong disorders of random flux γ. It is found that even a relatively large disorder does not alter the form of the soliton significantly.

Figure 4 shows the calculation results of the depinning current. The solid line with $\gamma = 0$ corresponds to the pinning force in a discrete system without disorder. This non-zero pinning force has a fundamental origin in the discrete system and is due to the Peierls-Nabarro potential which vanishes for $a \to 0$.[21] The curves with higher values of γ correspond to the non-zero random fluxes ranging from small amplitude disorder $\gamma = 0.05$ to the maximum disorder at $\gamma = 1$.

Two regimes of soliton depinning can be distinguished depending on the discreteness value a. If the parameter a is rather large, i.e. $a > 1$, the depinning force is determined by a Peierls-Nabarro potential and the influence of the randomly trapped fluxes is negligible. In this regime, the depinning current decreases with $1/a$. Arrays of the smaller discreteness or, more precisely, $a \lesssim 0.3$, however, exhibit an interesting regime where the depinning current I_{dep} *increases* as a function of $1/a$. Here, the Peierls-Nabarro potential is negligible and the pinning potential for the fluxon is due to the randomly trapped magnetic fluxes.

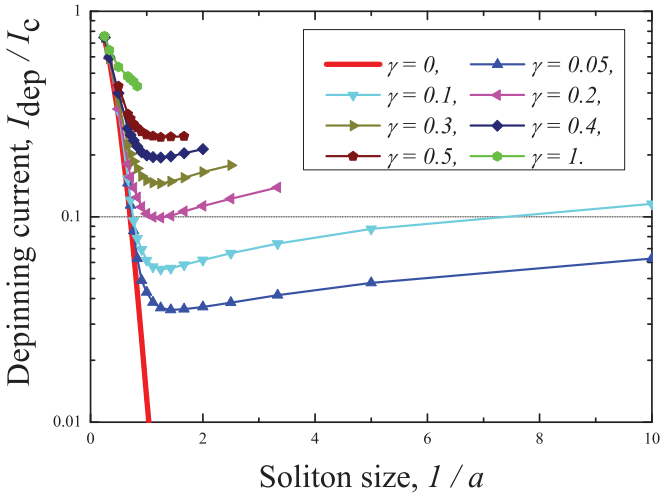

FIG. 4. (Color online) Dependence of depinning currents (voltages for charge case) on the inverse discreteness parameter $1/a$ for diverse strengths of disorder. The red line for $\gamma = 0$ shows the depinning current caused by the Pierles-Nabarro potential $\alpha \exp(-\beta/a)$ only, with $\alpha = 6$, $\beta = 5.6$.

It is interesting that the behavior of depinning force is a non-monotonic function of the discreteness a. Below a certain value of a (which varies with the amplitude of the disorder), the depinning force increases with $1/a$. This is explained by the fact that Φ_i and Q_i remain independent of the discreteness of the array a. In this case, the standard deviations of the phase ϕ_i and the charge variable q_i increase according to (4) and (8), leading to an increase of the potential barrier for the pinned soliton. Hence, a non-monotonic behavior of depinning force is a fingerprint of the kind of the disorder considered, e.g. static random "topological charges".

V. THEORY

Next, we provide the quantitative analysis of the soliton pinning as a function of its size and the magnitude of spatial disorder. The following analysis is valid for both dual charge and flux limits discussed above. Here, it will be applied to a parallel Josephson junction array in the presence of strong magnetic inhomogeneities, i.e. random magnetic fluxes. Since the most interesting regime is characterized by the condition $a \leqslant 1$, we consider the depinning of a single fluxon in a long Josephson junction, i.e. in the continuous limit of a Josephson parallel array. In this limit the long Josephson junction is equivalent to a Josephson parallel array. The total magnetic energy of the junction subject to an external bias current I can be expressed as:

$$E = E_J \int dx \left\{ \frac{1}{2}\left[\frac{d\varphi(x)}{dx}\right]^2 - \cos\left[\varphi(x) + \int_0^x \frac{dy}{a}\frac{\pi\Phi(y)}{\Phi_0}\right] - \frac{I}{I_c}\varphi(x) \right\}, \quad (9)$$

where E_J is the Josephson energy of the junction, I_c is the critical current in the absence of inhomogeneities, and the coordinate x is normalized to λ_J. In our particular model, the random magnetic flux distribution is characterized by a random function $\Phi(x)$ correlated to a small distance a. As the

inhomogeneities are considered to be not too strong (a more precise condition will be obtained later), a standard expression for the shape of a soliton can be used:

$$\varphi_0(x - x_0) = 4 \arctan e^{-(x-x_0)}, \tag{10}$$

where x_0 is the position of its center. Substituting Eq. (10) into Eq. (9) the soliton pinning force $F(x_0) = -\partial E/\partial x_0$ results as

$$F(x_0) = \frac{I_c}{2\pi} \int dx \frac{d\varphi_0(x-x_0)}{dx} \sin\left[\varphi_0(x-x_0) + \int_{x_0}^{x} \frac{dy}{a} \frac{\pi \Phi(y)}{\Phi_0}\right]. \tag{11}$$

Since the average value of $F(x_0)$ is zero, we define the average depinning current as $\langle I_{\rm dep}\rangle = \sqrt{\langle F^2\rangle}$, where the sign $\langle ...\rangle$ means the averaging over the inhomogeneities. A similar procedure was used in Ref. 18 to analyze the depinning current in long Josephson junctions with weak inhomogeneities. Thus, we obtain

$$F^2(x_0) = \left(\frac{I_c}{2\pi}\right)^2 \int \frac{dxdy}{2} \frac{d\varphi_0(x-x_0)}{dx} \frac{d\varphi_0(y-x_0)}{dy} \times \cos\left[\varphi_0(x-x_0) - \varphi_0(y-x_0) + \int_x^y \frac{dz}{a} \frac{\pi \Phi(z)}{\Phi_0}\right]. \tag{12}$$

The random function appearing in Eq. (12) is averaged as follows:

$$\left\langle \cos\left[\int_x^y \frac{dz}{a} \frac{\pi \Phi(z)}{\Phi_0}\right]\right\rangle = \prod_{n=1}^{L/a} \Re e \int_{-\gamma\pi}^{\gamma\pi} \frac{d\xi_n}{2\gamma\pi} \exp\left[i \sum_{k=x/a}^{y/a} \xi_k\right]. \tag{13}$$

Here, we assume that the normalized random fluxes $\xi_i = \pi\Phi_i/\Phi_0$ are uniformly distributed within the range $-\gamma\pi$ and $\gamma\pi$. Calculating the integrals over ξ_n yields

$$\left\langle \cos\left[\int_x^y \frac{dz}{a} \frac{\pi \Phi(z)}{\Phi_0}\right]\right\rangle = \exp\left[-\frac{\eta|x-y|}{a}\right], \tag{14}$$

where the parameter η is determined by the strength of the inhomogeneities γ:

$$\eta = \left|\ln \frac{\sin \pi\gamma}{\gamma\pi}\right| \simeq \frac{\pi^2\gamma^2}{6}. \tag{15}$$

Thus, we finally obtain the average value of $\langle F^2\rangle$ as

$$\langle F^2\rangle = \left(\frac{I_c}{2\pi}\right)^2 \int \frac{dxdy}{2} \frac{d\varphi_0(x)}{dx} \frac{d\varphi_0(y)}{dy} \cos[\varphi_0(x) - \varphi_0(y)] \times \exp\left[-\frac{\eta|x-y|}{a}\right]. \tag{16}$$

An explicit expression of $\langle F^2\rangle$ can be found by the Fourier transformation of Eq. (16)

$$\langle F^2\rangle = \left(\frac{I_c}{2\pi}\right)^2 \frac{2\pi\eta}{a} \int_{-\infty}^{\infty} dp \left[\mathrm{sech}^2\left(\frac{\mathrm{p}\pi}{2}\right) + \mathrm{cosech}^2\left(\frac{\mathrm{p}\pi}{2}\right)\right] \frac{\mathrm{p}^4}{\mathrm{p}^2 + (\eta/\mathrm{a})^2}. \tag{17}$$

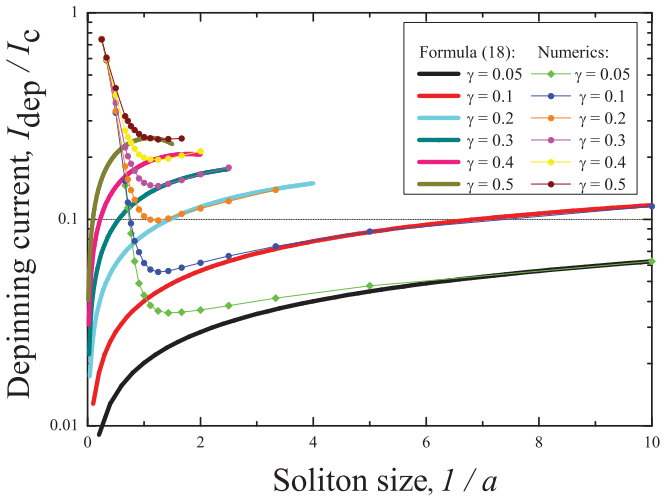

FIG. 5. (Color online) Comparison between numerical calculations of depinning currents and analysis, using formula (18) for different amplitudes of disorder. The Peierls-Nabarro potential is not taken into account.

Taking into account that all calculations are valid within the limit of $\eta/a \ll 1$ where the fluxon does not change its form, the integral over p in Eq. (17) can be calculated and the depinning current is obtained as follows:

$$I_{\rm dep}/I_c = \frac{1}{\pi}\sqrt{\frac{2\eta}{a}\left[1 - \frac{\eta}{a}\right]}, \quad \eta \leqslant a \leqslant 1. \tag{18}$$

The dependence of the depinning current on the soliton size $1/a$ shows an increase that is similar to that previously obtained in numerics. The numerics and basic formula (18) are compared in Fig. 5. As expected, the analysis works well only for small discreteness values a. An agreement with numerical simulations is rather good for large $1/a$.

In order to improve the analysis, the discreteness-induced Peierls-Nabarro's pinning force in the form of $\alpha \exp(-\beta/a)$ (where α and β are numerical parameters, obtained through the fitting procedure) could be added to the disorder-induced depinning part with the fitting coefficient f in (18) to make the analysis work also in the area of large discreteness:

$$I_{dep}/I_c = \frac{f}{\pi}\sqrt{\frac{2\eta}{a}\left[1 - \frac{\eta}{a}\right]} + \alpha \exp(-\beta/a) \tag{19}$$

As can be seen from the fit made in Fig. 6, formula (19) with $\alpha = 6$, $\beta = 5.6$, and $f \sim 0.8$ qualitatively describes the behavior of the depinning force in the range of discreteness parameter $a \lesssim 1$. It is necessary to mention that this formula with the corresponding fitting coefficients deviates from the limit expression $I_{dep}/I_c = 1 - \frac{\pi^2}{2a^2}$,[21] which is valid for the case $a \gg 1$. This is due to the initial restriction of our analysis to the regime of medium-to-small discreteness.

There is another intriguing and important fact characterizing the soliton's behavior in the junction array with static inhomogeneities. Some depinning curves in Fig. 4 end earlier than others. This corresponds to the situation when the disorder becomes so strong that a single soliton cannot exist inside the array. In the numerical calculations, this situation manifests itself by multiple solitons emerging inside the array. The spatial

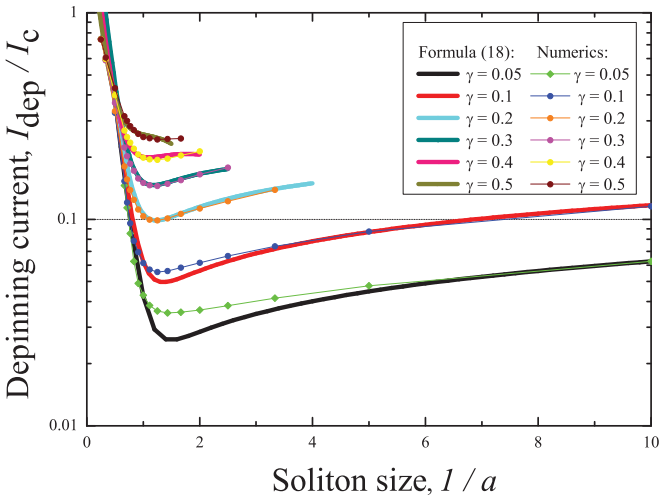

FIG. 6. (Color online) Comparison between numerical calculations of depinning currents and analytics, using formula (19) for different amplitudes of disorder. The Peierls-Nabarro potential is taken into account.

dependence of phase (charge variable) becomes extremely irregular and the ansatz of single soliton depinning is irrelevant. This gives the lower limit of the discreteness value a, which depends on the strength of disorder γ. This threshold can be estimated roughly by the condition of strong fluctuations $a_{\rm thr} = \eta$ and (15), which yields:

$$a_{\rm thr} = \frac{\pi^2\gamma^2}{6}. \qquad (20)$$

One of the important assumptions for the above results is the absence of correlations of random fluxes (Abrikosov vortices) or background charges in the neighboring cells. This means that all results obtained are valid only when the distance between junctions d is larger than the London penetration depth (for the flux case) or, for the charge case, than the charge screening length in a substrate. In the latter case, the charge screening length distance is roughly of the order of 10 nm for a weakly doped semiconductor substrate. The presence of non-local correlations would lead to a smoother spatial disorder in the array and facilitates depinning of solitons.

VI. CONCLUSIONS

We have studied the depinning of solitons in the discrete sine-Gordon system with spatial disorder. The results obtained apply to both fluxons in parallel arrays of Josephson junctions and Cooper pair solitons in series arrays of small Josephson junctions. The dependence of depinning force on both the discreteness parameter a and the disorder strength γ was investigated. The considered disorder corresponds to randomly trapped fluxes in a parallel Josephson array and background charges in a series array. It was found that for a fixed magnitude of disorder increase of the soliton size first leads to a decrease of the pinning force, but then starts to grow as shown in Fig. 4. Moreover, for arrays close to the continuous limit, single solitons become unstable under the influence of disorder.

We would like to thank A. Shnirman, H. Rotzinger, D. Haviland, and A. Zorin for stimulating discussions. K. Fedorov and A. Ustinov acknowledge the financial support by the SCOPE project and DFG via CFN project B3.6. M. Fistul acknowledges the financial support under SFB 491.

*kirill.fedorov@kit.edu

[1] T. A. Fulton and R. C. Dynes, Solid State Commun. **12**, 57 (1972).
[2] A. V. Ustinov, Physica D **123**, 315 (1998).
[3] V. P. Koshelets, S. V. Shitov, L. V. Filippenko, and A. M. Baryshev, Appl. Phys. Lett. **68**, 1273 (1996).
[4] D. E. Kirichenko and I. V. Vernik, IEEE Trans. Appl. Supercond. **15**, 296 (2005).
[5] D. V. Averin, K. Rabenstein, and V. K. Semenov, Phys. Rev. B **73**, 094504 (2006).
[6] Z. Hermon, E. Ben-Jacob, and G. Schön, Phys. Rev. B **54**, 1234 (1996).
[7] P. Delsing, K. K. Likharev, L. S. Kuzmin, and T. Claeson, Phys. Rev. Lett. **63**, 1861 (1989).
[8] D. B. Haviland and P. Delsing, Phys. Rev. B **54**, R6857 (1996).
[9] J. Bylander, T. Duty, and P. Delsing, Nature **434**, 361 (2005).
[10] M. Pierre *et al.*, Eur. Phys. J. B **70**, 475 (2009).
[11] I. V. Yurkevich, J. Baldwin, I. V. Lerner, and B. L. Altshuler, Phys. Rev. B **81**, 121305 (2010).
[12] A. J. Manninen and J. P. Pekola, Czech. J. Phys. **46**, 2293 (1996).
[13] L. G. Aslamazov and E. V. Gurovich, JETP **40**, 746 (1984).
[14] M. V. Fistul, JETP **69**, 209 (1989).
[15] M. V. Fistul, JETP Lett. **49**, 95 (1989).
[16] M. V. Fistul and G. F. Giuliani, Phys. Rev. B **56**, 788 (1997).
[17] V. M. Vinokur and A. E. Koshelev, JETP **70**, 547 (1990).
[18] M. B. Mineev, M. V. Feigei'man, and V. V. Shmidt, JETP **54**, 155 (1981).
[19] A. V. Ustinov, Appl. Phys. Lett. **80**, 3153 (2002).
[20] E. Goldobin, D. Koelle, and R. Kleiner, Phys. Rev. B **66**, 100508 (2002).
[21] O. M. Braun and Y. S. Kivshar, *The Frenkel-Kontorova Model*, (Springer, Heidelberg, Berlin, 2004).
[22] A. B. Zorin, Phys. Rev. Lett. **96**, 167001 (2006).
[23] S. V. Lotkhov, V. A. Krupenin, and A. B. Zorin, IEEE Trans. Instrum. Meas. **56**, 2 (2007).
[24] S. Rachel and A. Shnirman, Phys. Rev. B **80**, 180508(R) (2009).
[25] W. Guichard and F. W. J. Hekking, Phys. Rev. B **81**, 064508 (2010).